Monatshefte für Chemie 133, 909–918 (2002)

Monatshefte für Chemie
Chemical Monthly

Probing the Exciton Density of States in Semiconductor Nanocrystals Using Integrated Photoluminescence Spectroscopy

Sergey A. Filonovich[1], **Yurii P. Rakovich**[1], **Mikhail I. Vasilevskiy**[1], **Mikhail V. Artemyev**[2], **Dmitrii V. Talapin**[3], **Andrey L. Rogach**[3], **Anabela G. Rolo**[1], and **Maria J. M. Gomes**[1,*]

[1] Department of Physics, University of Minho, P-4710-057 Braga, Portugal
[2] Physico-Chemical Research Institute, Belarussian State University, 220000 Minsk, Belarus
[3] Institute of Physical Chemistry, University of Hamburg, D-20146 Hamburg, Germany

Summary. We present the results of a comparative analysis of the absorption and photoluminescence excitation (PLE) spectra *vs.* integrated photoluminescence (IPL) measured as a function of the excitation wavelength for a number of samples containing II–VI semiconductor nanocrystals (NCs) produced by different techniques. The structure of the absorption and PL spectra due to excitons confined in NCs and difficulties with the correct interpretation of the transmittance and PLE results are discussed. It is shown that, compared to the conventional PLE, the IPL intensity plotted against the excitation wavelength (IPLE spectra) reproduce better the structure of the absorption spectra. Therefore, IPLE spectroscopy can be successfully used for probing the quantized electron-hole (e-h) transitions in semiconductor nanocrystals.

Keywords. UV/Vis spectroscopy; Nanostructure; Exciton; Absorption.

Introduction

Within the last decades, the optical properties of small semiconductor particles have been intensively studied in order to obtain information on the energies and dynamics of photo-generated charge carriers as well as on the nature of the emitting states [1–4]. The electron-hole (e-h) energy levels of NCs can be determined from the analysis of the corresponding absorption spectra. However, measuring the optical absorption in films containing semiconductor nanocrystals becomes impossible if the substrate is opaque. Even if it is transparent, the collective effects in composite films with high NC fraction or *Rayleigh* scattering on film inhomogeneities often mask absorption peaks due to the quantized e-h transitions. In this work, we will demonstrate this by simple calculations and give experimental evidence of such effects in the transmittance of films containing II–VI semiconductor NCs. Also, we will show that the integrated (over a certain wavelength region) photoluminescence (PL) of NCs, measured as a function of the excitation wavelength,

* Corresponding author. E-mail: mjesus@fisica.uminho.pt

reproduces with high accuracy the shape of the absorption spectra if the latter is not obscured by other factors.

Results and Discussion

Absorption spectra modelling

Using the standard optics relations for a film on a transparent substrate, one can routinely obtain the absorption spectrum from the transmittance spectrum. The analysis of the absorption spectra can provide a way for determination of the energy spectrum of e-h pairs in NCs. Unfortunately, thin films produced by dropping NC solution onto the substrate are quite inhomogeneous in thickness (which is also hard to determine, because there are no interference fringes seen in the transmittance spectra). Unable to extract reliably the absorption, we noted that the reflectance of the films does not deviate much from unity and worked in terms of $-\log(\text{transmittance})$. Figure 1 shows experimental spectra of two *PMMA* films and one matrix-free film containing CdSe NCs in different concentration.

The modelling of the experimental spectrum of the most diluted film was performed as follows. First, the lowest absorption peak energy was taken from the spectrum. It was considered as the energy of the ($1S_e$–$1S_{3/2}$) e-h state in a

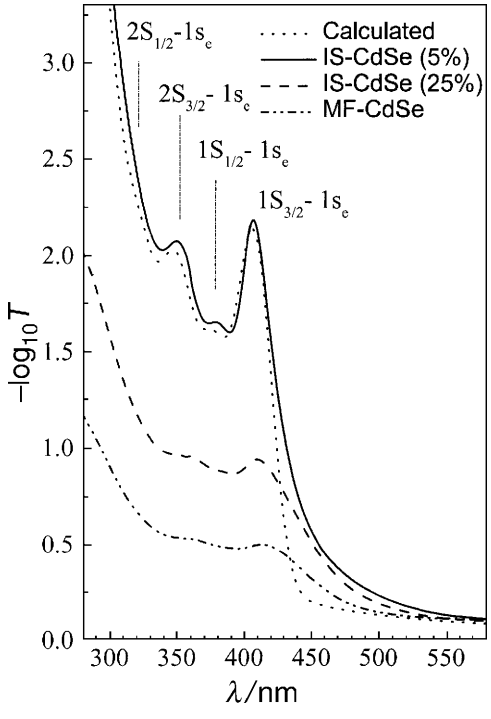

Fig. 1. Logarithm of the experimentally measured optical transmittance of two films containing CdSe NCs embedded into a *PMMA* matrices with different volume fraction and one matrix-free (MF) NC film; the theoretical curve is the optical density which was calculated assuming *Gaussian* distribution of radii (mean radius 16 Å, standard deviation 0.6 Å) and homogenous broadening of 20 meV; the film thickness was fitted

quantum dot (QD) of the most probable radius $\bar{R}$. This radius was calculated from the value of $E_1(R)$ using the effective mass approximation (EMA) [10]. Then, the energy of the ($1S_e$–$1S_{3/2}$) state for a QD of any radius R was calculated according to Eq. (1) where E_g is the bulk band gap energy, $E_{cor} = -0.248E_x$, and ε_0 and E_x are the dielectric constant and bulk exciton binding energy.

$$E_1(R) = \left(E_1(\bar{R}) - E_g - E_{cor} + 1.8\frac{e^2}{\varepsilon_0 \bar{R}}\right)\left(\frac{\bar{R}}{R}\right)^2 + E_g + E_{cor} - 1.8\frac{e^2}{\varepsilon_0 R} \quad (1)$$

Secondly, the polarizability of a QD of radius R was calculated using Eq. (2).

$$A = R^3 \frac{\varepsilon_\infty - \varepsilon_h + 4\pi\chi_{ef}(R)}{\varepsilon_\infty + 2\varepsilon_h} \quad (2)$$

$$\chi_{ef}(R) = \frac{3\varepsilon_h}{\varepsilon_\infty + 2\varepsilon_h}\chi(R);\ \chi(R) = \frac{e^2P^2}{m_0^2\omega^2 v}\sum_{\substack{\text{e-h}\\ \text{states}}}\frac{B_n}{E_n(R) - \hbar\omega - i\Gamma} \quad (3)$$

In Eqs. (2) and (3), ε_∞ and ε_h are the high frequency dielectric constants of the QD and matrix materials, respectively, e and m_0 are the free electron charge and mass, P is the dipole moment matrix element for the bulk semiconductor, ω is the frequency, $v = (4\pi/3)/R^3$ the QD volume, $E_n(R)$ the energy of the n^{th} e-h state calculated according to Eq. (1), Γ is the homogeneous broadening parameter, and

$$B_n = g_n\left|\int \psi_e^{(n)}\psi_h^{(n)}d\vec{r}\right|^2 \quad (4)$$

In Eq. (4), g_n is the degeneracy factor for the n^{th} e-h state, and $\psi_e^{(n)}$ and $\psi_h^{(n)}$ are the corresponding electron and hole EMA wavefunctions.

Given the QD polarizability A, the effective dielectric function was calculated as the third step of the spectra modelling procedure. For the film containing 5% of QDs, the modified *Maxwell-Garnett* formalism was employed which takes into account the distribution of QD radius [11]. The fitting parameters were the width of the size distribution (taken *Gaussian*), the homogeneous broadening parameter, and the film thickness. The result of these calculations presented in Fig. 1 is in quite a good agreement with the experimental spectrum.

In many cases, the absorption peaks in the spectra of films containing QDs are almost undistinguishable. A remarkable example of this is shown in Fig. 1. NCs used for preparation of all three films were synthesized in the same solution, *i.e.* were exactly the same. They differ only by NC concentration and thickness (this is why the most diluted film looks the less transparent). Why can the absorption peaks hardly be seen in the spectra of the higher NC concentration films?

One possibility is to attribute this to the dipole–dipole interaction between NCs polarized by the light. Such an effect has been observed in the FIR spectral region for dense NC films [12]. The dipole–dipole interaction can be taken into account within a well-known mean-field approximation called the *Bruggemann* model. Unfortunately, it has not been possible to include correctly the size dispersion in this scheme. Figure 2 shows what happens to the absorption when the concentration of single-size QDs increases. The peaks corresponding to the quantized e-h transition become broader and weaker and shift to the lower energy side.

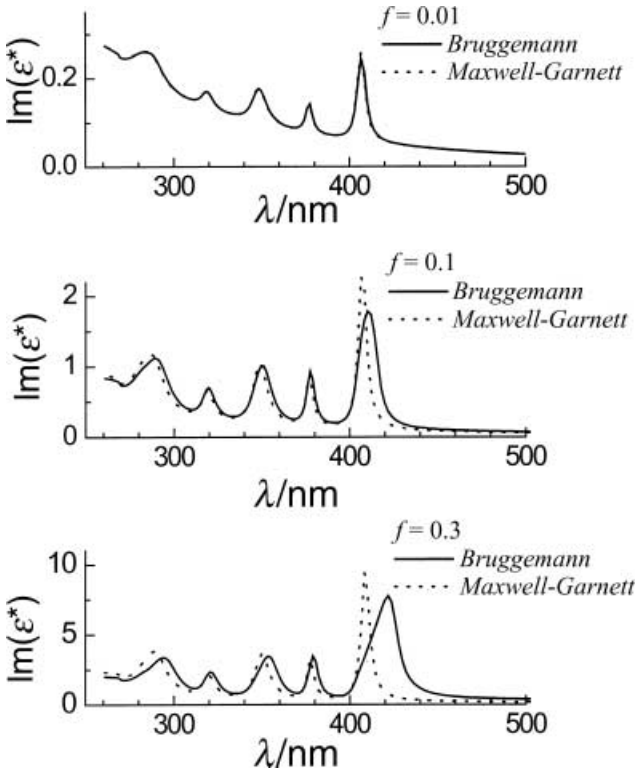

Fig. 2. Imaginary part of the effective dielectric function calculated using the modified *Bruggemann* and *Maxwell-Garnett* formalisms for ensembles of $R = 16$ Å CdSe QDs of different concentration; the QD parameters are the same as for the calculated spectrum in Fig. 1

Another probable reason is elastic light scattering. QDs by themselves are too small to produce significant scattering of visible light. However, they have a tendency to form aggregates in colloidal solutions and films. A simple calculation outlined below shows how the *Rayleigh* scattering can 'mask' absorption features originating from the quantized e-h transitions. First, we fitted one of the experimental spectra as explained above. Then, some *Rayleigh* scattering was assumed, which produces an extinction given by Eq. (5) (see *e.g.* Ref. [13]) where V is the volume of the inhomogeneities responsible for the scattering (for example, QD aggregates), p is the volume fraction of the inhomogeneities, and ε_1 and ε_2 are the real parts of the dielectric functions of the inhomogeneities and matrix, respectively. The former were taken as individual QDs of mean radius.

$$\gamma = \frac{4}{9} V \left(\frac{\omega}{c} \right)^4 p(1-p)(\varepsilon_1 - \varepsilon_2)^2 \tag{5}$$

The extinction according to Eq. (5) was then added to the absorption α to give an 'apparent' absorption coefficient:

$$\tilde{\alpha} = \alpha + \gamma \tag{6}$$

In Fig. 3, the calculated $\tilde{\alpha}$ spectra are shown for three values of the scattering volume. When it increases, the features in the spectrum fade out. We believe this

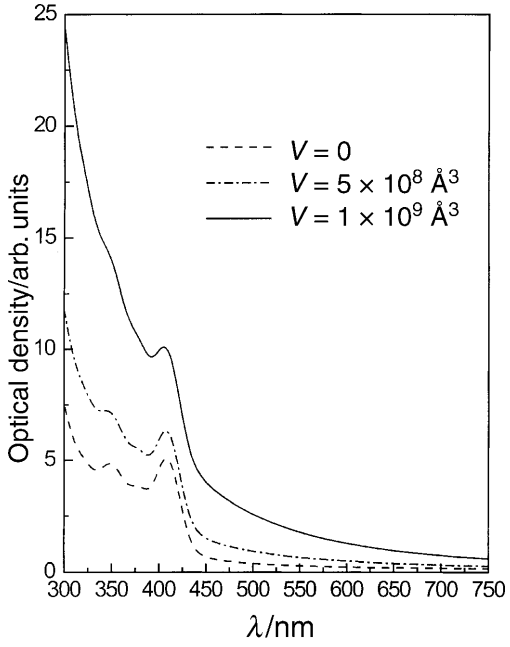

Fig. 3. Optical density spectra calculated with and without extinction (Eq. (5)); the scattering volume assumed in the calculation is given on the plot

could be the case of the higher NC concentration samples of Fig. 1, although the dipole–dipole interaction affecting real absorption was also present.

PL spectra

Let us now turn to the PL spectra shown in Fig. 4. The *Stokes* shift between the absorption and the emission for the CdSe/ZnS and the CdTe NCs was found as 31 and 104 meV, respectively. The full width of the PL band at half maximum is about 90 meV for the CdSe/ZnS nanoparticles and 155 meV for the CdTe NCs. These small shifts and widths of the PL band, which increased slightly with increasing incident photon energy, imply that the emission is due to the radiative recombination of $(1S_e{-}1S_{3/2})$ excitons in the QDs. We would like to emphasize that the PL spectra presented here were excited non-selectively, with the excitation light line intentionally broad to prevent possible size selection of the NCs. Under non-selective excitation conditions, the *Stokes* shift and PL line broadening originate mainly from the NC size distribution and fine structure of the $(1S_e{-}1S_{3/2})$ exciton state as discussed in Ref. [14]. Since the latter depends on the QD radius in a sophisticated way [14], it is rather difficult to extract the exciton density of states from the PL lineshape.

Assessing the density of states by PLE

It is well known that an absorption spectrum can be measured accurately only if the sample is sufficiently transparent, *i.e.* the condition $\alpha(\omega)d \ll 1$ must be satisfied (d is the sample thickness) [15]. As shown above, the measurement of real absorption

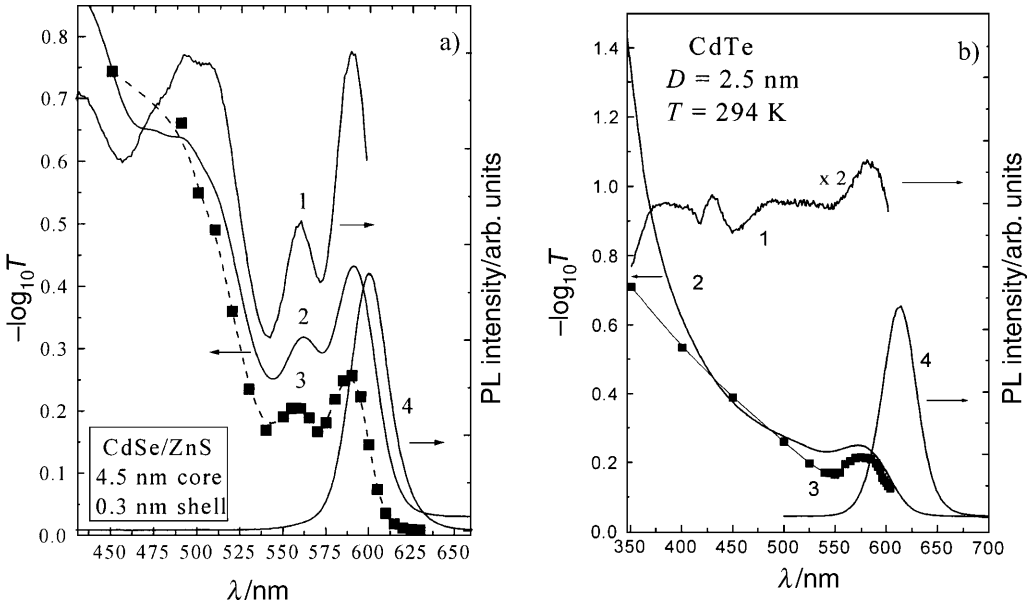

Fig. 4. PLE (1), $-\log T$ (2), IPLE (3), and PL (4) spectra of CdSe/ZnS (a) and CdTe (b) colloidal nanocrystals (T: transmittance)

can be problematic even for thin films because of the scattering and further effects. PLE spectroscopy has been generally accepted as a simple alternative in such cases. In this section, we will discuss the ability of the PLE technique for probing the density of confined excitonic states in samples containing QDs.

Measuring the PL intensity for a fixed photon energy (E_{PL}) and changing the excitation photon energy (E_{ex}), as it is usual in conventional PLE experiments [15], one should expect

$$I_{\mathrm{PL}} \propto I_{\mathrm{ex}} \cdot \int dR \left(g(R, E_{\mathrm{ex}}) F(R) P_{\mathrm{rel}} \frac{\Gamma_{\mathrm{PL}}}{\left(E_1(R) - E_{\mathrm{PL}} - \Delta(R)\right)^2 + \Gamma_{\mathrm{PL}}^2} \right), \qquad (7)$$

where P_{rel} is the probability of relaxation of a photogenerated e-h pair to the lowest excitonic state (E_1), $\Delta(R)$ is the *Stokes* shift between the absorption and emission in a QD of radius R, Γ_{PL} is a homogeneous broadening of the luminescence line, $F(R)$ is the QD size distribution function, and

$$g(R, E_{\mathrm{ex}}) \propto \sum_n \frac{B_{\mathrm{n}} \Gamma}{\left(E_{\mathrm{n}}(R) - E_{\mathrm{ex}}\right)^2 + \Gamma^2}$$

is the excitation probability for a QD of radius R. This function can be considered independent of R for E_{ex} within the first absorption peak, because the oscillator strength does not depend on the QD radius in the strong confinement regime. However, far from the absorption edge, $g \sim R^3$, since it is proportional to the number of participating e-h states.

Assuming that the excitation process does not depend significantly on R or E_{ex} (in other words, a photoexcited e-h pair always ends up at the lowest energy state), we can put $P_{\mathrm{rel}} = 1$. Under these conditions, PLE spectroscopy would yield a spectrum of the partial density of states due to NCs of some particular size

(determined by the chosen E_{PL}) and those whose size is most close to it. Such a spectrum can hardly be correlated to the absorption of the sample.

If instead of some fixed detection energy we choose to measure the PL intensity at the (variable) wavelength corresponding to the maximum of the PL band for each E_{ex}, we should obtain

$$I_{PL}(E_{ex}) \propto I_{ex} \cdot \int g(R, E_{ex}) F(R) \frac{\Gamma_{PL}}{\Delta^2 + \Gamma_{PL}^2} dR \tag{8}$$

Although the *Stokes* shift and broadening are both size dependent [14], Eq. (8) is a better approximation to the absorption. However, the most useful approach is to integrate over the excitonic PL lineshape,

$$\int I_{PL} dE_{PL} \propto I_{ex} \cdot \int g(R, E_{ex}) F(R) dR, \tag{9}$$

and plot the integrated PL against the excitation energy. The integral in the right-hand side of Eq. (9) is just the sample absorption (in the limit of low NC concentration). Hence, such an IPLE spectrum should give a good estimate of the shape of the absorption spectrum.

IPLE spectra

Guided by the reasoning presented above, we measured PLE (detected at the maximum of the PL band) and IPLE spectra of the films containing chemically prepared NCs (see Fig. 4). Although the PLE spectra clearly correlate with the first absorption peak, they do not follow the absorption spectra for higher energies. This is because only NCs of a certain size contribute to the emission at the maximum of the PL band. In other words, the luminescence lineshape depends on the excitation wavelength as already mentioned. At the same time, the integrated PL intensity plotted *vs.* the excitation wavelength reproduces with high accuracy the absorption spectra of the NCs (Fig. 4). The good correspondence obtained between the spectral position of the peaks in the absorption and IPL spectra confirms the origin of the observed PL band as the radiative recombination of e-h pairs confined in NCs of all sizes. Thus, we propose measurements of IPLE spectra as a method alternative to absorption spectroscopy. Arguments justifying this rely on the assumption of $P_{rel} = 1$ independently of the incident photon energy. Certainly, in some cases the luminescence efficiency can depend on E_{ex}, but it apparently does not for the samples of Fig. 4.

In order to demonstrate the usefulness of IPL spectroscopy, we investigated the photoluminescence properties of a Schott OG530 cut-off filter of 3 mm thickness. The CdS_xSe_{1-x} NCs in this sample are relatively large (*ca.* 12 nm in size), and x is nominally 0.7 [16]. Figure 5 shows the absorption, PL, PLE, and IPLE spectra of the sample. The PL spectrum consists of a broad low-energy (LE) band centred at 645 nm and a pronounced high-energy (HE) peak whose intensity depends on the excitation wavelength. The IPL intensity values (squares in Fig. 5) were obtained for certain excitation wavelengths by integrating over the spectral contour of the HE peak. The LE band is not directly related to confined excitons, and therefore it was not included in the integration procedure. Because of the high thickness of the

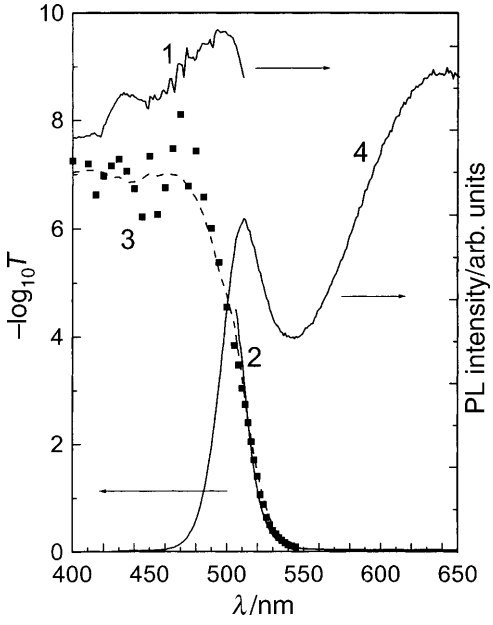

Fig. 5. PLE (1), optical density (2), IPL (3), and PL (4) spectra of OG530 glass filter; for IPL, points represent the calculated values and the line is guide to the eye

sample it is impossible to evaluate correctly the absorption from the transmission spectrum beyond 500 nm, whereas the IPLE (not the standard PLE!) allows for extrapolating the absorption spectrum up 450 nm. In the region of still shorter wavelengths, the behaviour of the IPLE spectrum becomes irregular, which manifests that the luminescence efficiency depends significantly on the excitation energy in this region. A possible reason for this can be the influence of electron or hole states (*i.e.* traps) located in the matrix or at the interface. Because of the large NC size, one should not expect noticeable confinement-related features in the absorption spectrum of this sample.

Conclusions

We measured the optical spectra of a set of samples containing II–VI nanocrystals. By modelling the absorption spectra of low NC concentration films, we were able to estimate the NC size dispersion and to evaluate the homogeneous broadening parameter. Possible reasons of smearing of the peaks in the absorption spectra are discussed. We showed that the PL intensity integrated over the excitonic PL band (rather than that measured at a fixed detection wavelength) plotted against the excitation wavelength is a function which can reproduce, under certain conditions, the absorption spectrum of a sample containing semiconductor NCs. It was demonstrated experimentally that the IPLE spectra indeed follow the absorption where the latter can be measured. It is therefore suggested that in many cases IPLE spectroscopy can be used for probing the exciton density of states in nanocrystals when direct measurements of the absorption are difficult either because of high thickness of the sample or significant extinction by film inhomogeneties.

Experimental

We studied several kinds of samples produced by different techniques. CdTe nanocrystals were prepared in the form of an aqueous colloidal solution. They were capped by a thioglycolic acid (*TGA*) shell, which made them air-stable and processable at ambient conditions. The details of the synthesis have been reported in Refs. [5, 6]. Briefly, 500 cm^3 of solution containing 0.013 *M* $Cd(ClO_4)_2$ and 0.02 *M TGA* were adjusted to *pH* 11.2 by addition of a 1 *M* solution of NaOH. Then, H_2Te gas obtained by decomposition of 0.8 g Al_2Te_3 with an excess of 0.05 *M* H_2SO_4 was passed into this solution in a nitrogen flow at room temperature. Subsequent heating of the reaction mixture at 100°C for different periods of time allowed to prepare colloids of CdTe nanocrystals with a mean particle size ranging from 2 to 6 nm and a particle size dispersion of about 10–15%.

CdSe and CdSe/ZnS core-shell nanocrystals were prepared as reported in Refs. [7, 8]. CdSe nanocrystals were synthesized *via* high-temperature thermolysis of Cd and Se organometallic precursors in a three-component mixture of hexadecylamine (*HDA*), tri-*n*-octylphosphine oxide (*TOPO*), and tri-*n*-octylphosphine (*TOP*). In a typical synthesis, 1 mmol of *TOP*Se, prepared according to Ref. [8], and 1.35 mmol of dimethylcadmium were dissolved in 5 cm^3 of *TOP* and rapidly injected into a vigorously stirred mixture of 10 g of *TOPO* and 5 g of *HDA* heated to 300°C. Further growth occurred at 250–310°C depending on the desirable NC size. To prepare CdSe/ZnS core-shell nanocrystals, the ZnS shell was grown onto the CdSe NCs. A solution of 0.4 mmol of diethylzinc and 0.51 mmol of bis-trimethylsilylsulfide in 3 cm^3 of *TOP* was introduced dropwise into a flask containing 2.5 cm^3 of the crude solution of CdSe NCs mixed with 5 g of *TOPO* and 2.5 g of *HDA* at 220°C.

Thin solid films of CdSe nanocrystals dispersed in a *PMMA* matrix were prepared as follows: CdSe NCs of a desired size were synthesized in *TOPO–TOP* as described above. Then, the NCs were precipitated with MeOH at room temperature and redissolved in $CHCl_3$ containing an appropriate amount of dissolved *PMMA*. Thin films of *PMMA* doped with CdSe NCs were prepared by casting from a $CHCl_3$ solution onto quartz glass and drying at room temperature [9]. Apart from the above mentioned samples we also studied some commercially available glass filters.

All transmission spectra were measured using a Shimadzu UV-3101 PC spectrometer. The PL spectra were recorded using a Spex Fluorolog spectrometer (1680-B monochromators with a dispersion of 1.70 nm/mm) equipped with a R943 Hamamatsu photomultiplier. The PL and PLE spectra were obtained by exciting the samples with a Xe lamp (output power: 0.1–2 mW depending on the wavelength; spot area: $\sim$10 mm^2).

Acknowledgements

This work was supported by the *Fundação para a Ciência e Tecnologia* (FCT, Portugal) through project PRAXIS/C/FIS/10128/1998 and SFB508 (Germany). *Y. P. Rakovich* and *S. A. Filonovich* acknowledge fellowships from PRAXIS XXI (FCT).

References

[1] Spanhel L, Haase M, Weller H, Henglein A (1987) J Am Chem Soc **109**: 5649
[2] Chestnoy N, Harris TD, Hull R, Brus LE (1986) J Phys Chem **90**: 3393
[3] O'Neil M, Marohn J, McLendon G (1990) J Phys Chem **94**: 4356
[4] Bawendi MG, Carrol PJ, Wilson W, Brus L (1992) J Chem Phys **96**: 946
[5] Rogach AL, Katsikas L, Kornowski A, Su D, Eychmüller A, Weller H (1996) Ber Bunsenges Phys Chem **100**: 1772
[6] Gao M, Kirstein S, Möhwald H, Rogach AL, Kornowski A, Eychmüller A, Weller A (1998) J Phys Chem B **102**: 8360
[7] Talapin DV, Rogach AL, Kornowski A, Haase M, Weller H (2001) Nano Lett **1**: 207
[8] Murray CB, Norris DJ, Bawendi MG (1993) J Am Chem Soc **115**: 8706

[9] Artemyev MV, Bibik AI, Gurinovich LI, Gaponenko SV, Woggon U (1999) Phys Rev B **60**: 1504
[10] Ekimov AI, Hache F, Schanneklein MC, Ricard D, Flytzanis C, Kudryavtsev IA, Yazeva TV, Rodina AV, Efros AL (1993) J Opt Soc America B **10**: 100
[11] Vasilevskiy MI, Akinkina EI, de Paula AM, Anda EV (1998) Semiconductors **32**: 11
[12] Vasilevskiy MI, Rolo AG, Artemyev MV, Filonovich SA, Gomes MJM, Rakovich YuP (2001) Physica Status Solidi B **224**: 599
[13] Landau LD, Lifshitz EM (1982) Electrodynamics of Continuous Media. Nauka, Moscow, p 582
[14] Efros AL, Rosen M, Kuno M, Nirmal M, Norris DJ, Bawendi M (1996) Phys Rev B **54**: 4843
[15] Klingshirn CF (1997) Semiconductor Optics. Springer, Berlin, p 403
[16] Persans PD, Tu AN, Lewis M, Driscoll T, Redwing R (1990) Mat Res Soc Symp Proc **164**: 105

Received October 16, 2001. Accepted (revised) January 7, 2002